Capillary Length in a Fluid−Fluid Demixed Colloid−Polymer Mixture

D. G. A. L. Aarts†

Van't Hoff Laboratory, Debye Research Institute, University of Utrecht, Padualaan 8, 3584 CH Utrecht The Netherlands

Received: December 14, 2004; In Final Form: February 4, 2005

We report measurements of the interfacial profile close to a vertical wall in a fluid−fluid demixed colloid−polymer mixture. The profile is measured by means of laser scanning confocal microscopy. It is accurately described by the interplay between the Laplace and hydrostatic pressure and from this description the capillary length is obtained. For different statepoints approaching the critical point the capillary length varies from 50 to 5 μm. These results are compared to theory. The mass density difference $\Delta\rho$ is calculated from the bulk phase behavior, which is described within free volume theory with polymers modeled as penetrable hard spheres. The interfacial tension γ is calculated within a squared gradient approximation. The capillary length is then given through $\sqrt{\gamma/g\Delta\rho}$ with g equal to the Earth's acceleration. Predictions from theory are in overall qualitative agreement with experiment without the use of any adjustable parameter.

I. Introduction

The study of colloid−polymer mixtures in the vicinity of walls is of fundamental as well as practical importance. Fundamental importance arises from the analogy between molecular fluid−fluid systems and phase separated colloid−polymer mixtures. In a classical paper, Vrij pointed out the importance and relevance of this analogy[1] (for a recent review, see ref 2). The origin of the phase separation in colloid−polymer mixtures lies in the polymer mediated colloid−colloid depletion attraction as first described by Asakura and Oosawa[3,4] and Vrij:[1] polymers are excluded from a region around the colloids for entropical reasons and two colloids within a certain distance of each other are effectively pushed together by the polymer osmotic pressure. In the present work, the coexisting phases are a colloidal liquid (rich in colloid and poor in polymer) and a colloidal gas (poor in colloid and rich in polymer). The resulting wetting behavior can be very rich and it recently gained attention from theory,[5,6] experiment,[7−10] and simulations.[11] Studying these systems close to walls is of practical importance as well. The food industry, for example, extensively uses the properties of both colloids and polymers to induce gelation or creaming[12,13] and walls clearly play an important role, e.g., in confining the products. Furthermore, in the living cell micro-compartmentation is often thought to be the result of phase separation, and it is evident that wetting properties play a crucial role in the equilibrium structure of the cell.[14]

Close to a vertical solid surface the interface between two fluids or between a gas and a liquid is curved. The exact shape of the interfacial profile (or meniscus) is determined by the interplay between the Laplace and the hydrostatic pressure. The characteristic length scale of the meniscus, the capillary length l_{cap}, is given by

$$l_{cap} = \sqrt{\frac{\gamma}{g\Delta\rho}} \tag{1}$$

with γ the interfacial tension, g Earth's acceleration and $\Delta\rho$ the mass density difference between the bottom and top phase. For molecular fluids the interfacial tension and the density difference are typically of the order of 10−100 mN/m and 0.1−1 g/mL, respectively, leading to a capillary length of $\sim$ 3 mm, which is for example the capillary length of water in contact with glass. In colloid−polymer mixtures γ is much smaller, since it has a typical magnitude proportional to[15,16]

$$\gamma \sim \frac{k_B T}{d^2} \tag{2}$$

where k_BT is the thermal energy and d the typical length scale, which is similar to the particle diameter far away from the critical point. This order of magnitude has been confirmed in experiment,[10,17−21] theory[5,6,22−24] and very recently in computer simulations as well.[25,26] For colloids that are about a hundred times larger than molecules, the capillary length thus becomes approximately a hundred times smaller, i.e., $\sim$30 μm.

In this work, the capillary length is measured in fluid−fluid phase separated colloid−polymer mixtures by analyzing the meniscus close to a vertical wall by means of laser scanning confocal microscopy for a number of state points along two dilution lines. In our experiment, the top fluid is rich in polymer and poor in colloid, the bottom fluid is poor in polymer and rich in colloid, and they will be referred to as a (colloidal) gas (G) and liquid (L), respectively. The measured capillary lengths are then compared with theory; the bulk phase behavior is described within free volume theory[27] with polymers modeled as penetrable hard spheres,[1] and the interfacial tension is calculated using a squared gradient (van der Waals) term. The goal of this work is to quantify the measured capillary length and compare to theory. Note that it is also possible to obtain the capillary length from the capillary wave spectrum as recently shown in ref 21, but this method is better suited for mixtures with larger colloids and thus even smaller interfacial tensions than presented here.

The paper is organized as follows. We will start with a description of the experimental methods in section II, followed by a theoretical consideration of the interfacial tension and the capillary length in section III. The results and the comparison

† Email: d.g.a.l.aarts@chem.uu.nl.

10.1021/jp044312q CCC: $30.25
Published on Web 03/22/2005

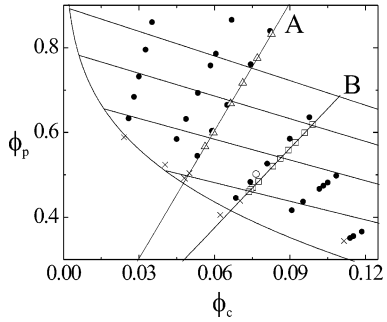

Figure 1. Phase diagram in (ϕ_p, ϕ_c)-representation. Indicated are points where gas−liquid-phase separation occurs (open and filled symbols), and statepoints in the one-phase region (crosses). The full curve is the theoretical binodal for the same q. Also indicated are several (theoretical) tielines. Lines A and B are two dilution lines along which the capillary lengths have been measured.

between experiment and theory will be presented and discussed in section IV. Concluding remarks are made in section V.

II. Experimental Methods

We prepared fluorescent poly(methyl methacrylate) (PMMA) colloidal spheres following the method of Bosma et al,[28] slightly modified by using *cis*/*trans*-Decalin (Merck, for synthesis) as reaction solvent (with density 0.88 g/mL). The (dynamic light scattering) radius R_c was 25 nm and the polydispersity was less than 10%, estimated from scanning electron microscopy images. The colloid density was 1.17 g/mL. As polymer commercially available polystyrene (Fluka) was used with a molecular weight $M_w = 233$ kg mol^{-1} ($M_w/M_n = 1.06$, with M_n the number-average molecular weigth) and a radius of gyration R_g of ∼14 nm (estimated from data in the literature[29]). The polymer density was 1.05 g/mL. In the 40% *cis*-/60% *trans*-Decalin mixture the Θ-temperature of the polystyrene polymer is about 16 °C,[29] whereas experiments were performed at room-temperature. Both species were dissolved in Decalin and since all densities were known, mass fractions could be directly converted to volume fractions of colloids, $\phi_c = 4/3\ \pi R_c^3 n_c$, and of polymers, $\phi_p = 4/3\ \pi R_g^3 n_p$, with n_c and n_p the number densities of colloids and polymers, respectively. Here, ϕ_p is thus the concentration relative to the overlap concentration. Note that since the colloidal system did not display a crystal phase, the colloid volume fractions have not been sealed on, for example, the freezing volume fraction. Samples were prepared by mixing colloid- and polymer-stock dispersions and diluting with Decalin. At high polymer concentrations it took a few hours before the system phase separated completely, at intermediate concentrations about 15 min and very close to the binodal again up to hours or even days.[30] The resulting macroscopic interface always was very sharp. In principle, the size ratio $q \equiv R_g/R_c = 0.56$ allows for the observation of gas, liquid and crystal phases[27] (section III), but only gas−liquid phase coexistence was observed. Fluid-crystal coexistence was possibly suppressed by the polydispersity of the spheres as is often seen in systems with small spheres and the system gelled instead of displaying a crystal phase at relatively high polymer concentrations. This observation can be related to recent theoretical predictions, which show that both sphere and polymer polydispersity favor gas−liquid coexistence and delay the onset of fluid−solid separation;[31,32] These predictions are valid for ideal polymers, but similar effects have been calculated for interacting polydisperse polymer chains on the level of gas−liquid-phase separation.[33]

In Figure 1, both the experimental and the theoretical phase diagrams are shown. The points stem from the experiment; the full curve is the theoretical binodal for gas−liquid-phase separation as will be explained in section III. Close to the critical point, phase separation becomes very slow, taking up to many days, which makes it unclear if the system is in the one or two phase region. Theoretical tie-lines—connecting coexisting states—are shown as well. In the calculation solid−fluid coexistence is ignored since it was not observed in experiment. At low volume fraction of colloids, the binodal is rather accurate. At higher concentrations, it lies just below where the experimental binodal would be expected. However, the theoretical binodal seems to be expanded to the right; i.e., the theoretical critical point lies at $\phi_c^{cp} = 0.20$, $\phi_p^{cp} = 0.16$, whereas the estimated experimental critical point lies at $\phi_c^{cp} \sim 0.1$, $\phi_p^{cp} \sim 0.36$. The reasons for this discrepancy are unknown.

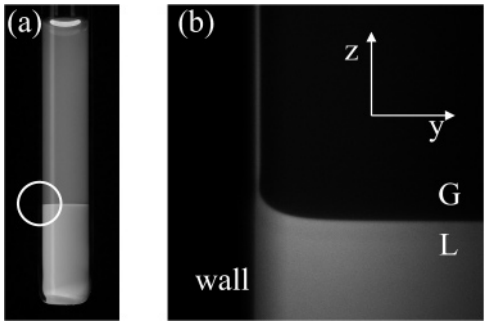

Figure 2. (a) Photograph of a phase separated mixture of fluorescently labeled PMMA colloids and polystyrene polymer in Decalin taken under UV light. (b) "Blow-up" of the encircled region in Figure 2a by means of LSCM (dimensions 350 μm by 350 μm).

To study the interfacial properties of the colloid−polymer mixtures laser scanning confocal microscopy (LSCM) was used. A confocal scanning head (Nikon C1) was mounted on a horizontally placed light microscope (Nikon Eclipse E400). Glass cells (of volume ∼ 1 cm^3) were used, both with and without stearyl-coated glass walls, which did not lead to essential differences, probably since the refractive index difference between solvent and colloids was very small and van der Waals interactions were thus minimal. The microscope detects the fluorescence of excited dye in the colloids, while solvent and polymers remain dark. Hence the colloidal rich phase (liquid) appears bright, whereas the colloidal poor phase (gas) appears dark.

After phase separation had completed, the interface looks very sharp by eye even close to a wall; see Figure 2a. Using a laser scanning confocal microscope (LSCM) enables one to resolve the details of the interfacial profile close to the wall, and in Figure 2b, the colloidal liquid phase is seen to favor the wall. In fact, the liquid phase even seems to wet the wall completely, although it is not yet clear whether the system is in true equilibrium (see for a more elaborate discussion[9]). Nonetheless, even during (the final stages of) phase separation the interfacial profile has a very similar shape, governed by the balance between the Laplace and the hydrostatic pressure, indicating that mechanical equilibrium rapidly sets in. Wijting et al.[7,8] used transmission light microscopy to study the interfacial profile in colloid−polymer mixtures, but the contour of the profile remained somewhat fuzzy.[8] Their focus was on the contact angle and no capillary lengths were measured. Clearly, LSCM has the advantage over light microscopy in that a thin slice can be imaged.[34]

III. Theory

In this section the capillary length is quantified theoretically from the density difference and the interfacial tension using (1).

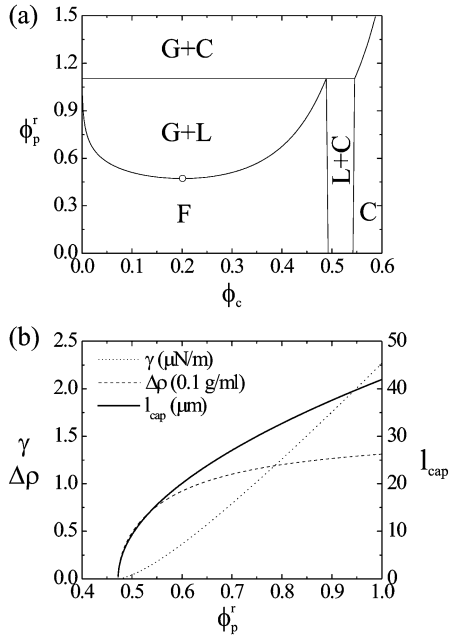

Figure 3. (a) Theoretical phase diagram of a colloid−polymer mixture with $q = 0.56$.[27] Shown are gas (G), liquid (L), fluid (F), and crystal (C) phases, as well as the critical point (open circle) and the triple point (horizontal line). (b) Interfacial tension, density difference (in units of 0.1 g/mL) and the resulting capillary length as a function of ϕ_p^r for the same colloid diameter $\sigma_c = 50$ nm as in the experimental system. More experimental details can be found in section II.

The colloid−polymer mixture is described as an effective one component mixture of attractive colloids.[27] The density difference follows directly from the bulk phase behavior which is obtained from free volume theory with polymers described as penetrable hard spheres.[27] To calculate the interfacial tension we use squared gradient theory (van der Waals theory) as described in more detail in ref 6. It is convenient to start with the thermodynamic potential $F(T, V, N_c, \mu_p^r)$ of a bulk fluid of N_c colloids in a volume V and with temperature T, in osmotic contact with a polymer reservoir of chemical potential μ_p^r. Using free volume theory,[27] we obtain in the case of ideal polymers

$$F(T, V, N_c, \mu_p^r) = F_0(T, V, N_c) - k_B T V \alpha n_p^r \qquad (3)$$

with $F_0(T, V, N_c)$ being the free energy of the pure hard sphere system. The Carnahan−Starling equation of state[35] is used to describe the fluid phase, whereas a free energy from computer simulations[36] is used for the crystal phase. The number density of polymers n_p^r in the reservoir becomes after multiplication by the free volume fraction α the number density of polymers in the system: $n_p \equiv n_p^r \alpha$. The key ingredient is this free volume fraction α, which is related to the accessible (free) volume for a polymer coil in a sea of N_c colloids. The free volume fraction depends for polymers as penetrable hard spheres only on the polymer to colloid size ratio $q \equiv R_g/R_c$, and on the colloid volume fraction ϕ_c: $\alpha = (1 - \phi_c) \exp[-Ad - Bd^2 - Cd^3]$, with $d = \phi_c/(1 - \phi_c)$ and $A = 3q + 3q^2 + q^3$, $B = 9/2\ q^2 + 3q^3$, and $C = 3q^3$. By application of common-tangent constructions, the bulk phase behavior can be calculated from (3) alone; see Figure 3a for $q = 0.56$, i.e., the experimental value of q. This phase diagram is in reservoir concentrations of polymer and can be readily converted to system concentrations of polymer as is done for the gas−liquid binodal; see the full curve in Figure 1. The above theory can be extended to include polymer−polymer interactions as shown in[37] but then the theoretical binodal will lie well above the experimental binodal, possibly because in experiment the polymer is still relatively close to θ-conditions (see section II).

To calculate the interfacial tension one needs to take the density inhomogeneities close to the interface into account, which is done here by including a squared gradient term in the density. This leads to the following density functional of the surface excess grand potential per unit area $\omega^{(s)}$

$$\omega^{(s)}[n_c] = \frac{F - \mu_c N_c + PV}{A} = \int_{-\infty}^{\infty} dz \left[f(n_c) - \mu_{coex} n_c + p_{coex} + m\left(\frac{dn_c}{dz}\right)^2 \right] \qquad (4)$$

which defines the interfacial tension, $\gamma \equiv \omega^{(s)}$. Here, μ_c is the colloid's chemical potential, P is the pressure, A is the area, z is the distance to the interface, $f(n_c) = F/V$ is the free energy density (eq 3), and μ_{coex} and p_{coex} are the colloid's chemical potential and pressure at coexistence, which do not depend on z. The square gradient coefficient m is given by the second moment of the direct correlation function. To calculate this term, we use the mean spherical approximation ranging only over the attractive part of the polymer mediated colloid−colloid interaction, similar to the approach followed in ref 23. For polymers as penetrable hard spheres, it leads to the following expression[6]

$$\frac{m}{k_B T \sigma_c^5} = \frac{\pi}{6} \phi_p^r \left[1 + \frac{7q}{4} + \frac{7q^2}{5} + \frac{7q^3}{10} + \frac{q^4}{5} + \frac{q^5}{40} \right] \qquad (5)$$

with $\phi_p^r = n_p^r\ 4/3\ \pi R_g^3$. Minimizing the functional (eq 4) with respect to n_c using functional derivation leads to

$$2m \frac{d^2 n_c}{dz^2} = \frac{df(n_c)}{dn_c} - \mu_{coex} \qquad (6)$$

which can be used to calculate the equilibrium interfacial tension:

$$\gamma = 2 \int_{n_{c,G}}^{n_{c,L}} dn_c \sqrt{m(f(n_c) - \mu_{coex} n_c + p_{coex})} \qquad (7)$$

which is independent of the interfacial density profile. Here, $n_{c,G}$ and $n_{c,L}$ are the number densities of colloids in the gas (G) and liquid (L) phase, respectively.

In Figure 3b, the interfacial tension γ from (7), the gas−liquid density difference $\Delta\rho$ directly obtained from Figure 3a and the capillary length l_{cap} from (1) are plotted as a function of volume fraction of polymer in the reservoir. Note that the prediction of the interfacial tension is in good agreement with density functional theory calculations by Brader et al.,[5] where the colloid−polymer mixture was described as a two-component system within fundamental measure theory. Furthermore, for homogeneous phases this density functional[38] reduces to the free volume theory,[27] such that the bulk phase behavior and the density difference found in the present work, will be found from the density functional theory as well. Approaching the critical point, we find that both γ and $\Delta\rho$ decrease according to their mean-field exponents (i.e., 1.5 and 0.5, respectively, in agreement with calculations by Brader and Evans[23]), leading to a decrease of the capillary length as well (with an exponent 0.5).

IV. Results and Discussion

The shape of the mensicus as shown in Figure 2b is described by the interplay between the Laplace and the hydrostatic

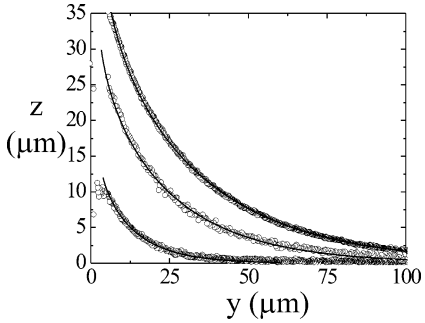

Figure 4. Interface from LSCM images as in Figure 2b (symbols) for three different statepoints (statepoints 3, 6, and 8 counted from top to bottom along dilution line B in Figure 1). The full curves follow from (8).

pressure. Close to the wall the disjoining pressure plays a role, but it turns out that no extra term is needed in the analysis. It leads to the following differential equation $\Delta\rho g z = \gamma/R(z)$ with $R(z)$ the radius of curvature at a distance z above the interface. In the case of a flat wall there exists an analytical solution[39]

$$\frac{y}{l_{cap}} = \left[\operatorname{arccosh}\left(\frac{2l_{cap}}{z}\right) - \operatorname{arccosh}\left(\frac{2l_{cap}}{h}\right) + \left(4 - \frac{h^2}{{l_{cap}}^2}\right)^{1/2} - \left(4 - \frac{z^2}{{l_{cap}}^2}\right)^{1/2}\right] \quad (8)$$

where y is the horizontal distance to the wall and $h = z$ ($y = 0$) the capillary rise. From the LSCM images as in Figure 2b, the meniscus can be easily determined as shown for three different state points in Figure 4. Next, the menisci are described by (8) with either l_{cap} and h as fitting parameters or -since the shape of the meniscus is solely determined by the capillary length- by again fitting to l_{cap} and now the wall position and assuming a certain height h, as explained in more detail in ref 10. Here, we followed the latter method, and (8) describes the data very accurately (Figure 4).

In Figure 5, the measured capillary lengths for the dilution lines shown in Figure 1 are shown as a function of the overall colloid volume fraction. Following the dilution line from high to low ϕ_c, tielines are crossed and the critical point is approached, although the dilution lines do not intersect this point. As a result the capillary length strongly decreases, but not all the way down to zero. The stars at the horizontal axes denote the first observations of stable colloid−polymer mixtures along dilution lines A and B, which are good indications of the location of the experimental binodal points that will lie just above the stars. The full curve follows from theory for the present experimental system and dilution lines. Clearly, the theoretical prediction is in qualitative agreement with experiment; the theoretical capillary length has the right order of magnitude and follows a similar shape as a function of the overall colloid volume fraction ϕ_c. Given the reasonable, but not perfect agreement between the theoretical and experimental binodal the differences are not surprising. In particular, the experimental data points in Figure 5b strongly decrease, since the dilution line intersects the experimental binodal relatively close to the experimental critical point, whereas the theoretical curve is calculated with respect to the theoretical critical point, which is more to the right in the phase diagram (see the discussion in section II).

To see from what properties the discrepancy between theory and experiment stems the density difference has been measured for one state-point ($\phi_c = 0.076$ and $\phi_p = 0.50$, open circle in Figure 1). The results are summarized in Table 1. The theoretical and experimental capillary length lie quite close together. However, both the theoretical density difference and interfacial tension overshoot the experimental measurements and these effects cancel to some extent. In particular, the discrepancy of the liquid densities is large, namely 0.050 g/mL in contrast with 0.002 g/mL for the gas densities (Table 1). This is a direct consequence of the apparent shift of the theoretical binodal as discussed in section II.

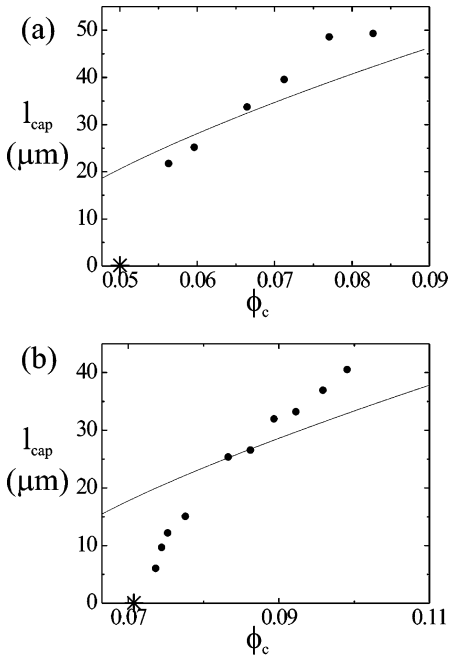

Figure 5. Capillary lengths for dilution lines A (a) and B (b) as a function of the overall concentration of colloids ϕ_c, see Figure 1. The symbols follow from measurements as in Figure 4 and the full curves directly stem from theory without any adjustable parameter. The stars at the horizontal axes denote the first observations of stable colloid−polymer mixtures along dilution lines A and B. The theoretical curves stop at the vertical axis at an overall ϕ_c where the experimental dilution line intersects the theoretical binodal.

TABLE 1: Comparison between Experiment and Theory

	l_{cap}	ρ_L	ρ_G	$\Delta\rho$	γ
experiment	18	0.942	0.889	0.053	0.16
theory	23	0.992	0.891	0.101	0.50

[a] The capillary lengths are in μm, the densities in g/mL and the interfacial tensions in μN/m. The experimental interfacial tension (obtained from the capillary length) is in good agreement with an analysis of the thermal capillary wave spectrum, following the method of ref 21, for which $\gamma \sim 0.2$ μN/m is obtained.

V. Concluding Remarks

We have shown precise measurements of the capillary length in colloid−polymer mixtures by analyzing the interfacial profile at a vertical hard wall. The profile is accurately described by the interplay between the Laplace and the hydrostatic pressure. The capillary lengths vary between 5 and 50 μm for different statepoints approaching the binodal. The experimental bulk phase behavior is reasonably well described by the theoretical prediction from free volume theory.[27] This is somewhat remarkable given the simple description of polymers as penetrable hard spheres. Furthermore, as shown in ref 6 predictions of the interfacial tension with squared gradient theory closely follow predictions by more sophisticated density functionals,[5] validating the use of squared gradient theory. From the phase behavior

and the interfacial tension the capillary length is readily obtained and there is overall qualitative agreement with the experimental data points. A more detailed comparison for a single statepoint shows that theory overestimates both the density difference and the interfacial tension. These effects cancel each other to some extent when calculating the capillary length. The difference between experimental and theoretical densities is a direct consequence of the mismatch between the experimental and theoretical binodal, whereas the mismatch itself indicates that the applied theory does not completely capture all the details of the experimental system. This leads to the difference between experimental and theoretical interfacial tension as well. It is unclear what details of the colloid−polymer mixture have to be included in theory to obtain a more quantitative agreement with experiment. One may think of taking polymer−polymer interactions into account. Several theories are available in the literature that provide a more realistic description of the polymer when calculating the phase behavior (see the reviews of this[2,40−42] and references therein) and the interfacial tension[6,24,43] of colloid−polymer mixtures. This might improve overall agreement between theory and experiment, but here we have kept the description as simple as possible. Given the overall qualitative agreement with experiment without the use of any adjustable parameter, we feel that the essential physics is included in the presented theory.

Acknowledgment. It is a pleasure to thank Roel Dullens for particle synthesis, Henk Lekkerkerker for stimulating discussions, and Remco Tuinier and Matthias Schmidt for critically reading the manuscript. This work was supported by the Stichting voor Fundamenteel Onderzoek der Materie (Foundation for Fundamental Research on Matter), which is part of the Nederlandse Organisatie voor Wetenschappelijk Onderzoek (Netherlands Organization for Advancement of Research).

References and Notes

(1) Vrij, A. *Pure Appl. Chem.* **1976**, *48*, 471−483.
(2) Poon, W. C. K. *J. Phys.: Condens. Matter* **2002**, *14*, R859-R880.
(3) Asakura, S.; Oosawa, F. *J. Chem. Phys.* **1954**, *22*, 1255−1256.
(4) Asakura, S.; Oosawa, F. *J. Polym. Sci.* **1958**, *33*, 183−192.
(5) Brader, J. M.; Evans, R.; Schmidt, M.; Löwen, H. *J. Phys.: Condens. Matter* **2002**, *14*, L1−L8.
(6) Aarts, D. G. A. L.; Dullens, R. P. A.; Lekkerkerker, H. N. W.; Bonn, D.; van Roij, R. *J. Chem. Phys.* **2004**, *120*, 1973.
(7) Wijting, W. K.; Besseling, N. A. M.; Stuart, M. A. C. *Phys. Rev. Lett.* **2003**, *90*, 19610.
(8) Wijting, W. K.; Besseling, N. A. M.; Stuart, M. A. C. *J. Phys. Chem. B.* **2003**, *107*, 10565−10570.
(9) Aarts, D. G. A. L.; Lekkerkerker, H. N. W. *J. Phys.: Condens. Matter* **2004**, *16*, S4231.
(10) Aarts, D. G. A. L.; van der Wiel, J. H.; Lekkerkerker, H. N. W. *J. Phys.: Condens. Matter* **2003**, *15*, S245−S250.
(11) Dijkstra, M.; van Roij, R. *Phys. Rev. Lett.* **2002**, *89*, 208303.
(12) Lorén, N.; Alstkär, A.; Hermansson, A. M. *Macromolecules* **2001**, *34*, 8117.
(13) Dickinson, E.; Walstra, P. *Food colloids and polymers: stability and mechanical properties*; Royal Society of Chemistry: Cambridge, U.K., 1993.
(14) Walter, H.; Brooks, D. E. *FEBS Lett.* **1995**, *361*, 135.
(15) Rowlinson, J. S.; Widom, B. *Molecular theory of capillarity.* Clarendon Press: Oxford, U.K., 1982.
(16) De Gennes, P. G. *Scaling concepts in polymer physics.* Cornell University Press: Ithaca, NY, 1979.
(17) Vliegenthart, G. A.; Lekkerkerker, H. N. W. *Prog. Colloid Polym. Sci.* **1997**, *105*, 27.
(18) de Hoog, E. H. A.; Lekkerkerker, H. N. W. *J. Phys. Chem. B* **1999**, *103*, 5274−5279.
(19) Chen, B. H.; Payandeh, B.; Robert, M. *Phys. Rev. E* **2000**, *62*, 2369−2372.
(20) de Hoog, E. H. A.; Lekkerkerker, H. N. W. *J. Phys. Chem. B* **2001**, *105*, 11636−11640.
(21) Aarts, D. G. A. L.; Schmidt, M.; Lekkerkerker, H. N. W. *Science* **2004**, *304*, 847.
(22) Vrij, A. *Physica A* **1997**, *235*, 120−128.
(23) Brader, J. M.; Evans, R. *Europhys. Lett.* **2000**, *49*, 678−684.
(24) Moncho-Jorda, A. Rotenberg, B.; Louis, A. A. *J. Chem. Phys.* **2003**, *119*, 12667.
(25) Vink, R. L. C.; Horbach, J. *J. Chem. Phys.* **2004**, *121*, 3253.
(26) Vink, R. L. C.; Horbach, J. *J. Phys.: Condens. Matter* **2004**, *16*, S3807.
(27) Lekkerkerker, H. N. W. Poon, W. C. K.; Pusey, P. N.; Stroobants, A.; Warren, P. B. *Europhys. Lett.* **1992**, *20*, 559−564.
(28) Bosma, G.; Pathmamanoharan, C.; de Hoog, E. H. A.; Kegel, W. K.; van Blaaderen, A.; Lekkerkerker, H. N. W. *J. Colloid Interface Sci.* **2002**, *245*, 292−300.
(29) Berry, G. C. *J. Chem. Phys.* **1966**, *44*, 4550.
(30) Aarts, D. G. A. L.; Dullens, R. P. A.; Lekkerkerker, H. N. W. *New J. Phys.* **2005**, *7*, 40.
(31) Fasolo, M.; Sollich, P. *J. Phys.: Condens. Matter* **2005**, *17*, 797.
(32) Fasolo, M.; Sollich, P. cond-matt/0410374, 2004.
(33) Paricaud, P.; Varga, S.; Cummings, P. T.; Jackson, G. *Chem. Phys. Lett.* **2004**, *398*, 489.
(34) Wilson, T. *Confocal Microscopy*; Academic Press Limited: London, 1990.
(35) Carnahan, N. F.; Starling, K. E. *J. Phys. Chem.* **1969**, *51*, 635.
(36) Frenkel, D.; Ladd, A. J. C. *J. Chem. Phys.* **1984**, *81*, 3188.
(37) Aarts, D. G. A. L.; Tuinier, R.; Lekkerkerker, H. N. W. *J. Phys.: Condens. Matter* **2002**, *14*, 7551−7561.
(38) Schmidt, M.; Löwen, H.; Brader, J. M.; Evans, R. *Phys. Rev. Lett.* **2000**, *85*, 1934−1937.
(39) Batchelor, G. K. *An introduction to fluid dynamics.* Cambridge Univeristy Press: Cambridge, U.K., 1967.
(40) Fuchs, M.; Schweizer, K. S. *J. Phys.: Condens. Matter* **2002**, *14*, R239.
(41) Tuinier, R. Rieger, J.; de Kruif, C. G. *Adv. Coll. Interface Sci.* **2003**, *103*, 1.
(42) Likos, C. N. *Phys. Rep.* **2001**, *348*, 267.
(43) Moncho-Jorda, A.; Dzubiella, J.; Hansen, J. P.; Louis, A. A. Submitted for publication in *J. Phys. Chem. B* **2005**.